Journal of Physical Chemistry & Biophysics

Nikolopoulos et al., J Phys Chem Biophys 2014, 4:3
DOI: 10.4172/2161-0398.1000144

Research Article Open Access

Response of CR-39 Polymer Radon-Sensors via Monte-Carlo Modelling and Measurements

Dimitrios Nikolopoulos[1*], Sofia Kottou[2], Ermioni Petraki[1,3], Efstratios Vogiannis[4] and Panayiotis H.Yannakopoulos[1]

[1]Department of Electronic Computer Systems Engineering, TEI of Piraeus, Greece, Petrou Ralli & Thivon 250, GR122 44, Aigaleo, Greece
[2]Medical Physics Department, Medical School, University of Athes, Mikras Asias 75, GR11527, Goudi, Greece
[3]Department of Engineering and Design, Brunel University, Kingston Lane, Uxbridge, Middlesex UB8 3PH, London, UK
[4]Evangeliki Model School of Smyrna, Lesvou 4, GR17123, Greece

Abstract

International studies of radon indoors and in workplaces have shown significant radiation dose burden of the general population due to inhalation of radon (^{222}Rn) and its short-lived progeny (^{218}Po,^{214}Pb, ^{214}Bi, ^{214}Po). As far as atmospheric radon concerns, ^{222}Rn, is not necessarily in equilibrium with its short-lived progeny. For this reason, radon's equilibrium factor *F* was solved graphically as a function of the track density ratio $R=T_B/T_R$, namely of the ratio between the recordings of cup-type and bare CR-39 detectors. T_B was computed through special Monte-Carlo codes which were implemented for the calculation of the efficiency of bare CR-39 polymers, regarding their ability in sensing the alpha particles emitted by the decay of radon and its short-lived progeny. For a realistic approach, Monte-Carlo inputs were adjusted according to actual experimental concentration measurements of radon, decay products and *F* of Greek apartment dwellings. Concentration measurements were further utilized for the calculation of the unattached fraction, f_p, in terms of Potential Alpha Energy Concentration (PAEC, defined as the sum of the initial - per volume - energies of all alpha particles emitted due to the decay of radon and its short-lived progeny that are present within a certain amount of air). This was employed for the calculation of *F* in terms of ratio (A_4/A_0), where A_i represents the activity concentration of radon (i=0) and ^{214}Po (i=4) respectively. Measured and calculated values of F were plotted versus R. The results were fitted and checked with model's predictions.

Introduction

Radon (^{222}Rn) is a naturally occurring radioactive gas generated by the decay of radium (^{226}Ra) which is present in soil, rocks, building materials and waters [1]. Following the decay of radium, a fraction of radon emanates and migrates through diffusion and convection. After migrating, part of radon escapes to the atmosphere and waters, and, disintegrates to a series of short-lived decay products (progeny) (^{218}Po, ^{214}Bi, ^{214}Pb and ^{214}Po). Outdoor concentrations of radon and progeny are low (in the order of 10 $Bq.m^{-3}$). On the other hand, indoor concentrations are accumulated, as a result of geological and meteorological parameters, ventilation, heating, water use and building materials [1]. Due to indoor accumulation, radon and progeny are recognised as the most significant natural source of human radiation exposure [1] and the most important cause of lung cancer incidence except for smoking [1].

Radon and its short-lived progeny disintegrate through a- and b-decay. In specific ^{222}Rn undergoes a-decay with $\lambda_0=2.093\times10^{-6}$ s^{-1}, ^{218}Po a-decay with $\lambda_1=3{,}788\times10^{-3}$ s^{-1}, ^{214}Pb b-decay with $\lambda_2=4.234\times10^{3}$ s^{-1}, ^{214}Bi b-decay constant with $\lambda_3=5.864\times10^{-4}$ s^{-1} and ^{214}Po a-decay with $\lambda_4=4{,}234\times10^{3}$ s^{-1} [1,2]. In indoor environments ^{222}Rn, is not necessarily in equilibrium with its short-lived progeny and for this reason the equilibrium factor *F* serves as a fare compromise for identifying the status of equilibrium between parent ^{222}Rn and remaining short-lived progeny [1,2]. Continuous measurement of *F* is time-consuming and requires active instruments. Hence the time-integration of *F* prerequisites special apparatus and may not be easily employed in large-scale surveys. For this reason, several researchers investigated combined uses of bare and cup-enclosed Solid State Nuclear Track Detectors (SSNTDs) for long-term estimation of *F* [2-8]. This paper reviews the theoretical aspects of the topic and formulates an new approximation based Monte-Carlo simulation, actual measurements and related published data. The paper addresses issues of relating recordings of bare CR-39 SSNTDs with those of calibrated cup-type dosimeters

Theoretical aspects

Radon's equilibrium factor, *F*, is defined as the ratio of the equilibrium equivalent concentration of radon (A_e) over the actual activity concentration of radon in air (A_0), namely [1]:

$$F = \frac{A_e}{A_0} \quad (1)$$

Equilibrium equivalent concentration is determined by the following equation [1,9-14]

$$A_e = 0.106\cdot(A_1^a + A_1^u) + 0.513\cdot(A_2^a + A_2^u) + 0.381\cdot(A_3^a + A_3^u) \quad (2)$$

and hence

$$F = \frac{0.106\cdot(A_1^a + A_1^u) + 0.513\cdot(A_2^a + A_2^u) + 0.381\cdot(A_3^a + A_3^u)}{A_0} \quad (3)$$

Superscripts a and u distinguish the contribution of each one of the two states of radon progeny (attached, unattached), subscripts 1,2 and 3 correspond to ^{218}Po, ^{214}Pb and ^{214}Bi and A_0, A_i^x (x=a,u and i=1,2,3)

***Corresponding author** : Dimitrios Nikolopoulos, Department of Electronic Computer Systems Engineering, TEI of Piraeus, Greece, Petrou Ralli & Thivon 250, GR122 44, Aigaleo, Greece, Tel: +0030-210-5381560; Mobile: +0030-6977-208318; Fax: +0030-210-5381436; E-mail: dniko@teipir.gr; NikolopoulosDimitrios@gmail.com

Received March 29, 2014; **Accepted** May 22, 2014; **Published** May 24, 2014

Citation: Nikolopoulos D, Kottou S, Petraki E, Vogiannis E, Yannakopoulos PH. (2014) Response of CR-39 Polymer Radon-Sensors via Monte-Carlo Modelling and Measurements. J Phys Chem Biophys 4: 144. doi:10.4172/2161-0398.1000144

($Bq.m^{-3}$) represent measured concentrations of radon and progeny respectively.

Assuming radioactive disintegration, ventilation and deposition as the sole processes of removal of radon progeny in ambient air, A_i^x (x=a,u and i=1,2,3) can be calculated as [2,3]:

$$A_i^x = d_j \cdot A_{i-1}^x \quad (4)$$

Parameter d_j reported by Faj and Planninic [3] can be expressed as

$$d_j = \frac{\lambda_i}{\lambda_i + \lambda_v + f_i^a \cdot \lambda_i^{d,a} + \left(1 - f_i^a\right) \cdot \lambda_i^{d,u}} \quad (5)$$

Where λ_v represents the ventilation rate, $\lambda_i^{d,x}$ (x=a,u and i=1,2,3) is the deposition rate constant of attached and unattached progeny and

$$f_i^a = \frac{A_i^a}{\sum A_i^a + A_i^u} \quad (6)$$

is the attached fraction of progeny *i*. Neglecting the attachment of ^{214}Pb,^{214}Bi and ^{214}Po nuclei, *F* may be calculated as:

$$F = 0.105 \cdot d_1 + 0.516 \cdot d_1 \cdot d_2 + 0.380 d_1 \cdot d_2 \cdot d_3 \quad (7)$$

Faj and Planninic [3] calculated d_j as a function of λ_v employing the Carnado's formula. The solution enabled calculation of *F* as a function of λ_v, namely $F = F(\lambda_v)$. Similar approach has been followed previously as well [3,7,12,13,16,17].

In actual conditions, however, attachment of unattached progeny to aerosol and humidity particles may differ and this affects progeny concentrations A_i^x (x=a,u and i=1,2,3). According to recent publications [9,10], the deposition and attachment rate constants of attached and unattached progeny differentiate in high-humidity environments due to peaking of water droplets and for this reason, symbolisation $\lambda_i^{d,x}$ (x=a,u and i=1,2,3) was adopted. Presuming however only typical low-humidity ambient room environments under a Jacobian [12,13,15] steady-state with complete mixing, $\lambda_i^{d,u}$ and $\lambda_i^{d,a}$ can be considered approximately constant for indoor room conditions [3,4,7-9,11]. In such conditions attachment and deposition rates are equal between unattached and attached nuclei and hence, symbolisation $\lambda^{d,x}$ (x=a,u) could be employed. According to Porstendorfer *et al.* [13] in typical rooms no differences are usually addressed between ambient electrical charged and neutral progeny clusters in attaching to aerosols and and depositing to surfaces. Under this perspective, the deposition rates of attached and unattached progeny to surfaces are equal. Employing symbolisation of Porstendorfer *et al.* [13] the term $f_i^a \cdot \lambda^{d,a}$ of equation (5) represents the deposition rate of attached nuclei, namely

$$q^a = f_i^a \cdot \lambda^{d,a} \quad (8)$$

Where q^a is the symbol for the deposition rate of all attached progeny. Symbolising q^u the deposition rate of all unattached progeny it follows from (9) that

$$q^u = f_i^u \cdot \lambda^{d,u} \quad (9)$$

Assuming a steady-state Jacobian model and complete mixing, concentrations of attached and unattached nuclei can be calculated then as [13]

$$A_i^a = \frac{(1 - R_{i-1})\lambda_i \cdot A_{i-1}^a + X \cdot A_i^u}{\lambda_v + \lambda_i + q^a + X} \quad (10)$$

and

$$A_i^u = \frac{\lambda_i \cdot A_{i-1}^u + R_{i-1} \cdot \lambda_i \cdot A_i^a}{\lambda_v + \lambda_i + q^u + X} \quad (11)$$

Where R_i is the recoil fraction of progeny *i*, *X* is the attachment rate to aerosols and *i* =1,2,3. R_1 =0.8 while R_2=R_3=0 [1]. Employing (10) and (11) in (3), *F* can be calculated as a function of λ_v, $\lambda^{d,u}$, λ^{da} and *X*, namely $F = F(\lambda_v, \lambda^{d,u}, \lambda^{da}, X)$. The latter approximation was employed by Eappen *et al.* [7] upper and lower bounds for *F* as well as average modelled values and related uncertainties.

It is very important that both approaches for the calculation of A^x (x=a,u and *i*=1,2,3), namely equation (4) for Faj and Planninic and equations (10),(11) for Eappen *et al.* [2,3,7] yield to similar final approximations for the most probable relation of modelled values of *F* versus measured progeny concentrations A_i^x (x=a,u and i=1,2,3). This relationship can be employed for the determination of *F* versus the recording efficiency between bare and cup-type SSNTDs (*R*). According to Faj and Planninic (1991) [4] this relationship follows the exponential law

$$F = a \cdot e^{-b \cdot R} \quad (12)$$

where

$$R = \frac{T_B}{T_R} \quad (13)$$

And T_B , T_R are the recorded track density values of bare and cup-enclosed SSNTDs. Similar were also the results reported by other investigators [3,4,7,14] Figure 1 presents the best approximations of *F* versus *R* according to the model of Faj and Planninic and according to the model of Eappen *et al.* [7] (Jacobi's model). Excellent coincidence is observed for all values of *R*.

Theoretical and Experimental Techniques

Theoretical approach

Let's assume a twin CR-39 detector system, namely a bare CR-39 SSNTD and another enclosed in a cup. The detector inside the cup records tracks attributable to time integrated ^{222}Rn concentration and the detector outside records tracks due to both ^{222}Rn and its progeny. While radon's concentration is unequivocally estimated, it is not so direct to estimate the progeny's equilibrium factor and PAEC from the track density of bare detectors. When the environment predominantly consists of radon and its progeny, a unique relationship as the one of equation (12) can be established between equilibrium factor values and the ratio of the cup to bare detector track densities [3-7,14,16-21].

Lets symbolise by T_R and T_B the track density values recorded on CR-39 by cup-type and bare detectors respectively. For calibrated CR-39 cup-type dosimeters, T_R will relate linearly to the concentration A_O of ^{222}Rn outside the cup. On the other hand, the track density T_B of bare CR-39's will be proportional to the ambient concentration of all a-emitting nuclei, namely to A_O of ^{222}Rn, A_1 of ^{218}Po and A_4 of ^{214}Po. If K_R and K_B are the sensitivity factors *tracks.cm^{-2} perBq.m^{-3}* of cup-type and bare CR-39 respectively, then

$$T_R = k_R \cdot A_0 \quad (14)$$

and

$$T_B = k_B \cdot (A_0 + A_1 + A_3) \quad (15)$$

Since $A_3 = A_4$. Equation (13), according to (14) and (15) can be written as

$$R = k \cdot (1 + r_1 + r_3) \quad (16)$$

where

$$k = \frac{k_B}{k_R} \quad (17)$$

is the sensitivity factor ratio, $r_1 = \frac{A_1}{A_0}$ and $r_3 = \frac{A_3}{A_0}$. Importantly, equation (17) calculates R from the concentration ratios r_1 and r_3.

According to equations (3), (16) and (17), if the concentrations A_i^x (x=a,u and i=1,2,3) are known from measurements, equilibrium factor $F = \frac{0.106 \cdot (A_1^a + A_1^u) + 0.513 \cdot (A_2^a + A_2^u) + 0.381 \cdot (A_3^a + A_3^u)}{A_0}$ can be calculated from measurement as well as from $r_3 = \frac{A_3}{A_0}$ and $r_3 = \frac{A_3}{A_0}$. If additionally the sensitivity factors k_B and k_R are known then k can be determined, and hence R. In this manner, the relationship between F and R can be established.

Experimental approach

In the framework of the NRSF Thalis Project of TEI of Piraeus, Greece, several active radon and progeny measurements have been conducted in Greek dwellings. Numerous measurements were performed with EQF3023 (EQF) of Sarad Instruments Gbhm. This instrument allows continuous 2-hour cycle measurement of radon and progeny nuclei, the latter discriminated for their attached or unattached mode. Radon's concentration is measured through ionisations produced within a chamber installed inside EQF by the alpha particles emitted during the decay of a radon's amount that is collected at the beginning of each cycle via 10-minute pumping. Progeny concentration is measured by two semi-conductor detectors at two stages. First, during the first hour of the 2-hour cycle, all alpha activity is collected by the first semiconductor either if this corresponds to unattached or attached progeny. Simultaneously, the second detector collects the unattached progeny nuclei that manage to transmit through a mesh-grid of 50 nm. Then, during the second cycle, the semiconductor detectors are interchanged, while, at this stage, the first remains in contact with a paper filter on which all plated out progeny are also measured. Through alpha-spectrographic techniques and proper mathematical analysis, as stated by the manufacturer's manual, all activities are determined. From the active database, several actual values of A_0 and A_i^x (x=a,u, i=1,2,3) were employed. From these additional value sets were calculated as averages at the 95% confidence interval, under the constraint of employing only partial values of a certain dwelling measurement-set during each calculation. From these actual A_i^x (x=a,u, i=1,2,3) measurement sets, equilibrium factor F values were calculated according to (3). Additionally, to this type of calculation, F was also derived from calculated values of the unattached fraction, f_p, in terms of PAEC as $f_p = \frac{PAEC_u}{PAEC_a + PAEC_u} = \frac{PAEC_u}{PAEC}$ where $PAEC^x = 3.690 * A_1^x + 17.830 * A_2^x + 13.120 * A_3^x$ (x=a,u, i=1,2,3). This was employed for the calculation of F in terms of ratio $\frac{A_1}{A_4}$ according to Doerschel and Piesch [14] where A_i represents the activity concentration of radon (i=0) and ^{214}Po (i=4) respectively.

Passive radon measurements within the Thalis Project are being conducted with a cup-type CR-39 dosimeter which was calibrated previously [15]. This cup-type dosimeter has well-established linear response to radon exposure. The sensitivity factor of this dosimeter has been experimentally defined and found equal to k_r = *(4.62 ± 0.33) (tracks.cm^{-2} perBq.m^{-3}.h)*. From the actual measurements of A_0, T_R was calculated according to (14).

Track density of bare CR-39 detectors was calculated by means of combining the real measurements of EQF with results derived via Monte-Carlo methods. More specifically, A_1 and A_3 were calculated from EQF measurements considering that $A_i = A_i^u + A_i^a$, i = 1,3. From these and the corresponding A_0 values, the concentration ratios were calculated as $r_1 = \frac{A_1}{A_0}$ and $r_3 = \frac{A_3}{A_0}$. Since k_B is not easily measurable, Monte-Carlo methods were employed for its determination. The following steps were followed:

1. The distance l travelled by alpha particles prior to hitting CR-39 was calculated versus alpha energy through SRIM2013 for the whole alpha-particle energy range of radon's decay chain. The relationship

$$l = R_{max} - (3.34773 \cdot E + 0.34937 \cdot E^2 + 0.02142 \cdot E^3) \quad (18)$$

was employed where R_{max} =*4.09cm* for alpha-particles originating from ^{222}Rn, R_{max} =*4.67cm* for alpha-particles originating from ^{218}Po and R_{max} =*6.78cm* for alpha-particles originating from ^{214}Po.

2. Random emission points of ^{222}Rn, ^{218}Po and ^{214}Po were generated around CR-39 and their travelling direction vectors were calculated.

3. From the direction vectors of (2), the hit data (l,θ_h,φ_h) were calculated.

4. For alpha-particles with l inside an effective volume, incident energy E_h was calculated from the reciprocal of (18) under the constraint $\theta_h \le \theta_{cr}$.

5. From hit data (E_h,θ_h,φ_h) the range and end points in CR-39 were

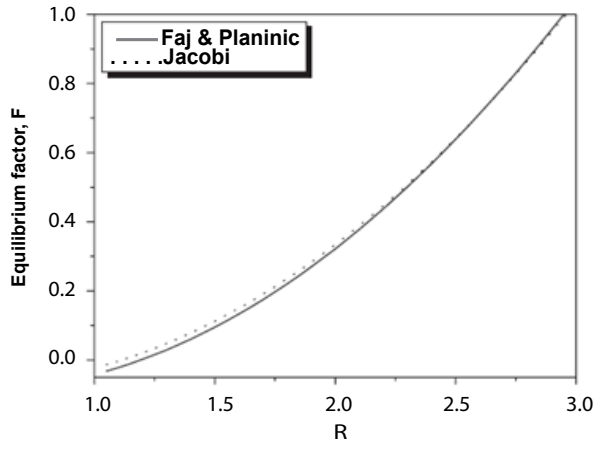

Figure 1: Relationship between equilibrium factor and the track ratio *R*.

calculated.

6. Steps (1)-(5) were iterated for N_0 particles of ^{222}Rn, ^{218}Po and ^{214}Po.

7. From steps (1)-(6) the number of recorded particles of ^{222}Rn, N_0^{rec}, of ^{218}Po, N_1^{rec} and of ^{214}Po , N_4^{rec} were calculated

To estimate realistic values of N_0 for ^{222}Rn, ^{218}Po and ^{214}Po (denoted as $N_{0,i}$) the following equation was employed

$$N_{0\,i} = A_i \cdot V_i \cdot t_{\exp} \tag{19}$$

where $A_i = A_i^u + A_i^a$, V_i is the sensitive volume's dimensions, t_{exp} is an assumed value for the exposure time (30 days) and *i=0,1,4*. From (19) and the Monte-Carlo output the recorded particles N_i^{rec}, *i=0,1,4* were calculated. From N_i^{rec} the track density of bare CR-39 detectors was calculated as

$$T_B = \frac{N_0^{rec} + N_1^{rec} + N_4^{rec}}{S} \tag{20}$$

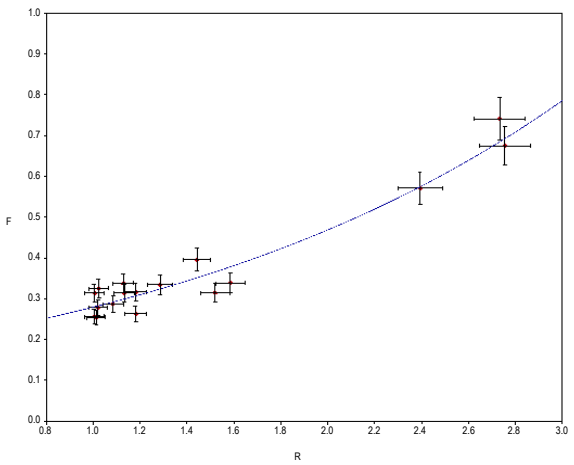

Figure 2: Relation of *F*, *R* according to Table 1

Table 1: *Characteristic value sets of F, R.*

Equilibrium Factor F	Ratio R
0.3384	1.5852
0.3137	1.1319
0.3379	1.1273
0.2562	1.0043
0.2865	1.0838
0.3148	1.5200
0.2540	1.0117
0.2628	1.1810
0.3249	1.0240
0.3137	1.0051
0.2781	1.0200
0.3345	1.2846
0.3957	1.4425
0.3164	1.1810
0.5709	2.3939
0.6748	2.7557
0.7413	2.7300

The results of Table 1 are presented graphically in Fig.2

Where *S* is the area of the employed CR-39 detectors, namely 1 cm^2.

From (20) the total sensitivity factor k_B of bare CR-39 detectors was calculated as

$$k_B = \frac{T_B}{(A_0 + A_1 + A_3)} = \frac{N_0^{rec} + N_1^{rec} + N_4^{rec}}{S \cdot (A_0 + A_1 + A_3)} \tag{21}$$

Outcomes and Discussion

Table 1 presents characteristic sets *F*, *R* according to the methodology already described. It may be recalled that the *F* values were calculated from experimental EQF measurements and that the *R* values were calculated from measurements and calculations.

The relationship between *F* and *R* has similarities to that of Figure 2. For this reason the data of Table 1 were fitted to the exponential model (12), namely to $F = a.e^{-b.R}$ Fitting gave a = 0.1663, b= -0.5165 with r^2=0.91. These data are in accordance to the published results of Faj and Planninic, Eappen *et al.* [3,4,7]. It is noted that the latter publication represents a critical review of the subject together with other results. Differences are due to differences in the sensitivity factor of the employed cup-type dosimeters of this study and those of the other studies. Indeed different geometries of cup-type dosimeters induce differentiations in detection efficiency due to alterations (a) in the field that the detectors face; (b) in the distribution of energies and incidence angles of alpha particles that hit the detector's surface or surfaces; (c) in radon's entrance properties e.g., diffusion, permeability etc.; (d) other reasons. The relationship between calculated values of *F* and *R* indicated non good fit to the exponential model (12) with r^2=0.51. This finding strengthens the integrity of the approximation followed in this paper, namely the "semi-empirical" modelling, viz., Monte-Carlo modelling fed with experimental measurements. Accounting the criticism of the method of Doerschel and Piesch [13] from several researchers [5,7,16-21] the fit result of calculated *F* values verified, more or less, this criticism. No other *F* -calculation approaches [6,7.14,18,21] were attempted, despite that some of these could provide better estimation of *F* -values. Nevertheless, the approach of this paper outweighs in one fact; the actual measurements of *F*. In addition, the overall Monte-Carlo modelling constitutes a new approach to previous simulations [16,18-26], most importantly, by taking into account the latest version of SRIM software, namely SRIM 2013. Apart from the work of Rezaie and Rezaie, *et al.* [22,23] which also used SRIM, all previous modelling for use of nuclear track detectors in long term estimation of *F*, followed completely other approximations [17,18] or mathematical-analytical models [16,24,25]. However, despite the different approximations, the findings of this paper could be useful for alternative long-term estimation of *F* or Monte-Carlo modelling of cup-type, bare detectors or other detector installations. This latter view, namely long-term estimation of *F*, was the final outcome of this work. Accounting the findings of this work, long-term measurements with CR-39 polymers will be implemented. Further work will simulate LR-115 polymers under similar semi-empirical modelling approach, expecting to implement a multi-sensor assembly of cup-enclosed and bare CR-39 and LR-115 polymers for long-term radon progeny measurements.

From the data of Table 1, sensitivity factors of bare CR-39 SSNTDs were calculated according to (21). Average k_B of this study was found equal to k_B = *(4.6 ± 0.6)(tracks.cm^{-2} perBq.m^{-3}.h).* This value does not differ significantly from the value of k_R. The latter implies from equation (17) that k $k \approx 1$. This finding is very important. Indeed, Faj and Planninic [3,4] assumed equal values for k_B and k_R. The present study verifies this result. Similar was also the outcomes of Eappen *et al.* [9]. Related publications gave also comparable results [5,6]. All

these findings could be explained by the fact that CR-39 registers alpha particles from radon and progeny identical either if enclosed in a cup or bare. Observed track density differences are attributable only to the fact that cup type CR-39 dosimeters are proportional to radon concentration only, while bare CR-39 SSNTDs register proportional to the concentrations of all alpha-emitters. Future work will employ other expressions of F namely those that take into account the the unattached fraction in terms of PAEC.

Conclusions

This study reported a newly developed Monte-Carlo simulation tool for modelling the CR-39 SSNTDs efficiency. Simulation combined Monte-Carlo techniques, experimental data and the latest version of SRIM (SRIM2013) software program group. This "semi-empirical" simulation perspective constitutes a completely new approach in SSNTD modelling. Modelling rendered calculation of sensitivity of CR-39 detectors based on energy and angular distributions of alpha-particles emitted by the decay of radon and progeny. The relationship between equilibrium factor F and recorded track density values ratio (of bare and cup-enclosed SSNTDs respectively), R, was additionally calculated through measurements and calculations. The sensitivity of bare CR-39 detectors was calculated equal to $k_B = (4.6 \pm 0.6)(tracks.cm^{-2}\ perBq.m^{-3}.h)$. This value is not significantly different from the corresponding sensitivity factor k_R of the cup-type dosimeters employed in this work. The ratio of for k_B and k_R was found approximately one, namely $k \approx 1$. This finding is considered as very important since it is verifies the results the similar studies. In addition, it also verifies the integrity of Monte-Carlo simulation and the overall mathematical approximations.

Acknowledgement

This research has been co-financed by the European Union (European Social Fund – ESF) and Greek national funds through the Operational Program "Education and Lifelong Learning" of the National Strategic Reference Framework (NSRF) - Research Funding Program: THALES Investing in knowledge society through the European Social Fund.

References

1. Nazaroff WW, Nero AV (1988) Radon and its Decay Products in Indoor Air. John Wiley & Sons, Inc., USA. ISBN 0-471-62810-7, 518.
2. Planinic J, Faj Z (1989) The equilibrium Factor F between Radon and its Daughters. Nucl Instrum Methods A 278: 550-552.
3. Planinic J, Faj Z (1990) Equilibrium factor and dosimetry of Rn by a nuclear track detector. Health Phys 59: 349-351.
4. Faj Z, Planinic J (1991) Dosimetry of radon and its daughters by two SSSN Detectors. Radiat Prot Dosim 35: 265-268
5. Amgarou K, Font L, Baixeras C (2003) A novel approach for long-term determination of indoor 222 Rn progeny equilibrium factor using nuclear track detectors. Nucl Instrum Methods Phys Res A 506: 186–198.
6. Abo-Elmagd M, Mansy M, Eissa HM, El-Fiki MA (2006) Major parameters affecting the calculation of equilibrium factor using SSNTD-measured track densities Radiat. Meas 41: 235-240.
7. Eappen KP, Mayya YS, Patnaik RL, Kushwaha HS (2006) Estimation of radon progeny equilibrium factors and their uncertainty bounds using solid state nuclear track detectors Radiat. Meas 41: 342-348.
8. Cliff KD, Wrixon AD, Green BM, Miles JC (1983) Radon daughter exposures in the U.K. Health Phys 45: 323-330.
9. Nikolopoulos D1, Vogiannis E (2007) Modelling radon progeny concentration variations in thermal spas. Sci Total Environ 373: 82-93.
10. Nikolopoulos D1, Vogiannis E, Petraki E, Zisos A, Louizi A (2010) Investigation of the exposure to radon and progeny in the thermal spas of Loutraki (Attica-Greece): results from measurements and modelling. Sci Total Environ 408: 495-504.
11. Nikolopoulos D1, Vogiannis E, Petraki E, Kottou S, Yannakopoulos P, et al. (2013) Dosimetry modelling of transient radon and progeny concentration peaks: results from in situ measurements in Ikaria spas, Greece. Environ Sci Process Impacts 15: 1216-1227.
12. Jacobi W (1972) Activity and potential alpha-energy of 222 radon-and 220 radon-daughters in different air atmospheres. Health Phys 22: 441-450.
13. Porstendorfer J1, Pagelkopf P, GrÃ¼ndel M (2005) Fraction of the positive 218Po and 214Pb clusters in indoor air. Radiat Prot Dosimetry 113: 342-351.
14. Doerschel B, Piesch E (1994) Effect of varying unattached fraction of radon daughters on the measurement of the equilibrium factor using nuclear etched track detectors. Rad Prot Dosim 541: 41-45.
15. Nikolopoulos D, Louizi A, Petropoulos N, Simopoulos S, Proukakis C (1999) Experimental study of the response of cup-type radon dosemeters. Radiat Prot Dosim 83: 263-266.
16. Nikezic D, Yu KN (2010) Long-term determination of airborne concentrations of unattached and attached radon progeny using stacked LR 115 detector with multi-step etching. Nucl Instrum Method A 613: 245-250.
17. Brown JM1, Solomon S, Tinker RA (2011) Development of an energy discriminate CR-39(Â®) nuclear track etch dosimeter for Radon-220 gas measurements. J Environ Radioact 102: 901-905.
18. Harley NH1, Chen J, Chittaporn P, Sorimachi A, Tokonami S (2012) Long term measurements of indoor radon equilibrium factor. Health Phys 102: 459-462.
19. Nikezic D (1994) Determination of detector efficiency for radon and radon daughters with CR-39 track detector a Monte Carlo study. Nucl Instrum Meth A 344: 406-414.
20. Sima O (2001) Monte Carlo simulation of radon SSNT detectors. Radiat Meas 34: 181-186.
21. Rehman FU1, Jamil K, Zakaullah M, Abu-Jarad F, Mujahid SA (2003) Experimental and Monte Carlo simulation studies of open cylindrical radon monitoring device using CR-39 detector. J Environ Radioact 65: 243-254.
22. Rezaie MR (2012) Calculating CR-39 Response to Radon in Water Using Monte Carlo Simulation. Iran J Med Phys 9: 193-201.
23. Rezaie MR, Sohrabi M, Negarestani A (2013) Studying the response of CR-39 to radon in non-polar liquids above water by Monte Carlo simulation and measurement. Radiat Meas 50: 103-108.
24. Yu KN, Leung SYY, Nikezic D, Leung JKC (2008) Equilibrium factor determination using SSNTDs. Radiat Meas 43: S357-S363.
25. Stajic J1, Nikezic D (2011) Hit probability of a disk shaped detector with particles with a finite range emitted by a point-like source. Appl Radiat Isot 69: 875-879.
26. Makelainen I (1984) Calibration of Bare LR-115 Film Radon Measurements in Dwellings. Radiat Prot Dosim 2: 195-197.